УДК 539.171

MODEL-INDEPENDENT DESCRIPTION OF THE LIGHT NUCLEUS-NUCLEUS ELASTIC SCATTERING AT INTERMEDIATE ENERGIES

V. Yu. Korda[1], A. S. Molev[1], L. P. Korda[2]

[1]*Institute of Electrophysics and Radiation Technologies, National Academy of Sciences of Ukraine, Kharkov*
[2]*National Science Center "Kharkov Institute of Physics and Technology", National Academy of Sciences of Ukraine, Kharkov*

We propose a new approach, based on the evolutionary algorithm, which enables to extract a scattering matrix $S(l)$ as a complex function of angular momentum l directly from the nucleus-nucleus elastic scattering data at intermediate energies without any additional model assumptions implied. Due to the automatic monitoring of the scattering matrix derivatives, the obtained S-matrix for ^{16}O - ^{16}O-scattering at 350 MeV is determined by the modulus and nuclear phase, which are smooth monotonic functions of angular momentum. We show the independence of the final S - matrix shapes of the primary model representations chosen to be the commonly used phenomenological ones.

1. Introduction

S-operator is a fundamental quantity of the scattering theory, which incorporates, by a general assumption, all possible information on any possible scattering process (including particle creation or destruction). In the case of elastic scattering, the diagonal matrix elements of S-operator in the angular momentum representation can be given in general form as

$$S(l) = \eta(l)\exp\left(2i\varphi(l)\right), \qquad (1)$$

where the S-matrix modulus $\eta(l)$ and the scattering phase $\varphi(l)$ are real, smooth functions of l. The unitarity of the S-matrix for the composite particle-nucleus scattering in the presence of nuclear absorption requires that $\eta(l) \le 1$, so we put

$$\eta(l) = \exp\left(-2\delta_a(l)\right), \qquad (2)$$

where the nuclear absorption phase $\delta_a(l)$ must be a real, smooth, positive function of l.

Since the colliding nuclei have electric charges, then the scattering phase $\varphi(l)$ can be divided into two parts

$$\varphi(l) = \delta_r(l) + \sigma_C(l), \qquad (3)$$

where the nuclear refraction phase $\delta_r(l)$ and the Coulomb scattering phase $\sigma_C(l)$ must be real, smooth functions of l.

From a general physics viewpoint, the only restrictions we may impose on the nuclear phases $\delta_{a,r}(l)$ to be determined are their finite values at small l, total vanishing at sufficiently large l and smooth behavior in the intermediate region. The most natural and simple approximation for $\delta_a(l)$ (or $\eta(l)$) and $\delta_r(l)$ is a monotonically descending (for $\eta(l)$, ascending to unity) function that can be easily modeled with the help of, say, Fermi-step or Gauss functions. For the case of elastic heavy-ion scattering at intermediate energies ($E \ge \ge 20$ MeV/nucleon), the S-matrix approaches of such a kind (see, e.g., [1 - 3]) and the optical potential models that yield $S(l)$ with such a behavior (see, e.g., [4, 5]) have appeared to be quite successful and argued for the so-called „rainbow" interpretation of the data. However, these models have not allowed an adequate description of all the features of the data measured.

The substantial improvement in the quality of fit is achieved with the help of more flexible $S(l)$ forms, which allow the phases to behave nonmonotonically for all relevant l. Such a nonmonotonic behavior is provided by extension of the standard (monotonic) S-matrices with the series of the pole-like terms (see, e.g., [6]) or the proper (say, spline) basis functions (see, e.g., [7, 8]). Similar behavior is inherent in the S-matrices calculated from the optical potentials that have the additional derivative-like interior terms or have the more complicated forms obtained by use of the spline functions or the Fourier - Bessel series (see, e.g., [5, 9, 10]). In spite of the excellence of the quality of fit provided in such approaches, the rainbow interpretation of the data appears to be no longer valid, which raises the problem of finding the physical meaning of the results obtained this way.

Clearly, all the approaches just mentioned are more or less model-dependent because the functions used to model the phases $\delta_{a,r}(l)$ and the real and imaginary parts of optical potential $V(r)$ and $W(r)$ are more or less the properly parameterized analytical ones. Thus, the search spaces of all possible shapes for the S-matrix and the optical potential are strongly reduced, and consequently data analyses performed on such spaces can lead to an incorrect physical interpretation of the data.

That is why it would be highly desirable to have the procedure that could extract the scattering matrix and/or the optical potential directly from the experimental data, without the introduction of any bias towards some *a priori* „physically reasonable" model assumptions. The very first question this procedure must answer to is whether the nonmonotonic (e.g. pole-like) structures and any other distortions, which appear in the *S*-matrix shapes obtained in the most successful approaches, are really necessary to reproduce the experimental data studied. This will help us to shed more light on the applicability of the rainbow interpretation to the heavy-ion collisions in the wide range of energies and mass numbers.

2. Model-independent determination of the scattering matrix

To develop the desired procedure which determines $S(l)$ directly from the data, we need to solve the problem in its most explicit form, in which each value of $\delta_{a,r}(l)$ is treated generally as an independent fitting parameter. This makes the problem parameter space highly dimensional and the choice of an appropriate search method crucial. Evolutionary (or genetic) algorithms (EAs) have many times proved very efficient in dealing with very difficult physical problems (see, e.g., [11, 12]), so we have chosen EA as a key element of our procedure.

According to the general ideology of the EA implementation, we deal with the population of *N* individuals. Each individual is the *S*-matrix presented as the pair of the real-valued $l_{\max}$ - dimensional vectors $[\delta_a(l), \delta_r(l)]$, l = 0, 1, ..., $l_{\max}$ - 1. The fitness of each individual reflects the quality of data fitting provided by the individual's *S*-matrix. By using the mutation operation the algorithm evolves the initial population of the badly fitted individuals to the final population of the highly fitted ones.

Every iteration of our procedure contains the following steps:

1. Generating the initial population of *N* individuals. For each individual the vectors $\delta_{a,r}(l)$ are filled with the help of any monotonically descending function of l, the first derivative of which has only one minimum. To be definite and to test the robustness of the procedure against various starting conditions, we choose the following three primary models for $S(l)$.

1). The six-parameter model composed of two Fermi functions

$$2\delta_i(l) = g_i f(l, l_i, d_i),$$

$$f(l, l_i, d_i) = \left[1 + \exp\left(\frac{l - l_i}{d_i}\right)\right]^{-1}, \; i = a, r. \quad (4)$$

2). The four-parameter model composed of two Gaussian functions

$$2\delta_i(l) = g_i \exp\left(-\frac{l^2}{d_i^2}\right). \quad (5)$$

3). The five-parameter McIntyre model [1]

$$\eta(l) = f(-l, -l_a, d_a),$$

$$2\delta_r(l) = g_r f(l, l_r, d_r). \quad (6)$$

The parameters g_i, l_i and d_i are positive. They are chosen for each individual and each model function at random within some intervals that are wide enough to produce substantially different shapes of the phases. Normally, all the individuals in a given population are initialized with one and the same function from the set (4) - (6). All the mentioned primary models for $S(l)$ are „physically justified".

2. Evaluating the fitness of each individual in the population. The fitness function in our approach consists of two parts. The first one is associated with the quality of the shapes of $\delta_{a,r}(l)$, and the second one accounts for the quality of the fitting of the experimental data.

The requirements that the shapes of $\delta_{a,r}(l)$ must meet in our approach are as follows:

i). The functions $\delta_{a,r}(l)$ must be descending.

ii). The first derivatives of $\delta_{a,r}(l)$ must have only one minimum and no maxima.

iii). The second derivatives of $\delta_{a,r}(l)$ must not have more than one minimum and one maximum.

iv). The third derivative of $\delta_r(l)$ must not have more than one minimum and one maximum.

v). The logarithmic derivative of $\delta_r(l)$ must be descending.

The requirements i) - iii) ensure the absence of any distortions of the phase shapes, at least up to the second-order derivatives. The condition iv) is added because we want the deflection function $\Theta(l) = 2d\varphi(l)/dl$ to have no shape distortions up to the same order of its derivatives. The condition v) provides for the permanent decrease of $\delta_r(l)$ with the increase of l. The requirements i) - iv) are crucial for the shapes of $\delta_{a,r}(l)$. Thus the penalties imposed on the individual in the case of violation of these requirements are fatal. The condition v) is not so

strong and introduces only the ultimate bias towards the desired tail of $\delta_r(l)$.

The quality of the fit of the calculated differential cross section to the experimentally measured one is assessed by means of the standard χ^2 magnitude per data point. The calculations are made by using the expansion of the scattering amplitude into a series of Legendre polynomials. The elastic scattering differential cross section is equal to the squared modulus of this amplitude.

It is often claimed that the amount of the large scattering angle data is insufficient to determine the scattering matrix and/or the optical potential in a unique way. Thus, we add several additional pseudo data points after the last actual ones, which follow the tendency of the cross section behavior (see, e.g., [8]). Of course, this prescription cannot be universal and must be used with care in the context of the data under study. The incorporation of the invented data points to the χ^2 criterion can appear misleading for the fitting procedure; therefore, we use the penalty-free corridor around those points and apply the prescription only after the fitting to the actual data set has been accomplished.

3. Letting each individual in the population produce *M* offsprings. The replication is performed according to the transformation

$$\log[\delta_i^{'}(l)] = \log[\delta_i(l)] + A_i N_i(0,1) D(l, l_{m,i}, d_{m,i}), \quad (7)$$

where $\delta_i(l)$ and $\delta_i^{'}(l)$ are the parent's and offspring's *S*-matrix phases, respectively, $i = a, r$, $A_i > 0$ is the mutation amplitude, $N_i(0,1)$ denotes a normally distributed one-dimensional random number with mean zero and one standard deviation, $l_{m,i}$ stands for the mutation point chosen randomly in the interval $0 \le l_{m,i} \le l_{\max}$ - 1, $d_{m,i} > 0$ is the value characterizing the diffuseness of the mutation region. The diffusing function $D(l, l_{m,i}, d_{m,i})$ must be of the bell-like shape with the only maximum at $l = l_{m,i}$ and the fall-off tail around this point.

To be definite and to ensure the proper localization of the consequences of the mutation we choose the diffusing function in the form

$$D(l, l_{m,i}, d_{m,i}) = \exp\left[-\frac{(l - l_{m,i})^2}{d_{m,i}^2}\right]. \quad (8)$$

The mutation amplitude A_i and the mutation diffuseness $d_{m,i}$ are the quantities automatically tuned within some intervals. The limits of these intervals, having the extremely large values at the beginning of the procedure, are smoothly decreased in the course of the run and acquire small values at the end. Such a schedule provides for both the removal of the features of the primary parameterizations (4) - (6) from the individual's $S(l)$ and the fine tuning of the details of $S(l)$.

4. Evaluating the fitness values of all offsprings. Sort the offsprings in descending order according to their fitnesses. Select *N* best offsprings to form the new population.

5. Going to step 3 or stopping if the best fitness in the population is sufficiently high (the χ^2 value is small enough).

EAs make up, generally, the global optimization technique that, however, cannot guarantee that the optimum found is the global one. Therefore, it is necessary to run the procedure several times. Besides, there is no way to know in advance what the minimum value of the χ^2 magnitude will be. Thus, it is instructive to monitor the dynamics of the best, worst and mean fitness values and the rms deviation from the mean fitness in the population during those several runs of the procedure. Such monitoring usually helps to localize the region of the potentially lowest χ^2 values.

3. Scattering matrix for elastic ^{16}O - ^{16}O-scattering at 350 MeV

We applied our technique to analyze the well-known test case of the elastic ^{16}O - ^{16}O-scattering at 350 MeV, for which the approaches that give a very good quality of fit predict the existence of the nonmonotonic structures in the *S*-matrix (see, e.g., [6, 7]).

In our calculations, bearing in mind that the collision energy is sufficiently high, we let $\sigma_C(l)$ in (3) to be the quasiclassical phase of the point-charge scattering by the uniformly charged sphere (see, e.g., [2]) having the radius $R_C = 0.95 \cdot 2 \cdot 16^{1/3}$ [13]. The calculated elastic scattering differential cross sections were symmetrized for the scattering of identical nuclei. The experimental errors were assumed to be equally weighted (10 % error bars).

Figs. 1 - 3 show the results of our calculations with the primary models (4) - (6) for $S(l)$, respectively. The χ^2 values for our fits to the data under consideration are 2.4 - 2.5. For each initial case, the results of five different runs of the procedure are presented to display the error bands within each of the primary $S(l)$ models. Fig. 4 compiles three best results from Figs. 1 - 3 to illuminate their sensitivity to the details of the particular primary $S(l)$ model. Fig. 5 demonstrates the consequences of the consideration of the invented data points in the region of large scattering angles.

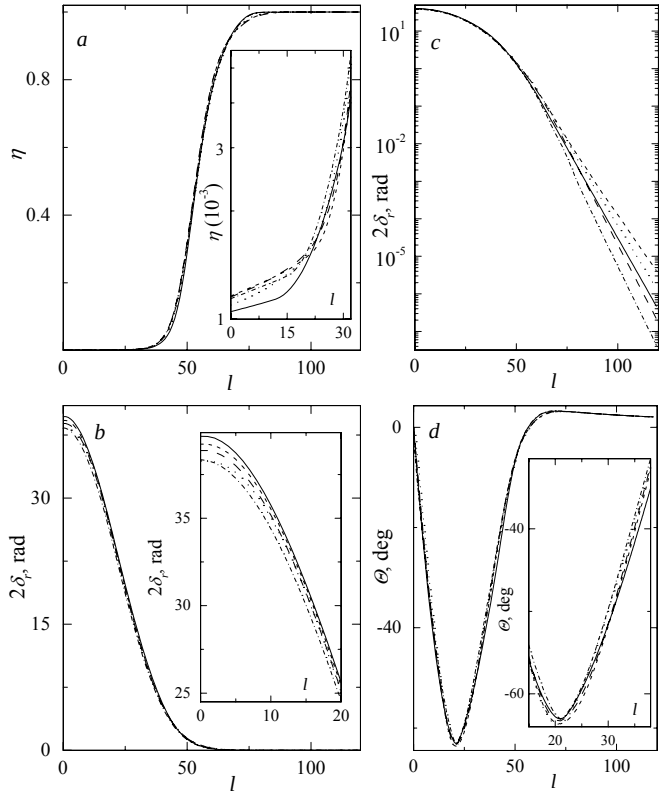

Fig. 1. Five scattering matrices for the elastic ^{16}O - ^{16}O-scattering at 350 MeV, calculated by our procedure with the primary model (4) for $S(l)$. *a* – the S-matrix moduli $\eta(l)$. The inset shows the region of small momenta in the logarithmic scale; *b* – nuclear phases $\delta_r(l)$. The inset shows the region of small momenta in the enlarged scale; *c* – the same as *b* but in the logarithmic scale; *d* – deflection functions $\Theta(l)$. The inset shows the vicinity of $\Theta(l)$ minima in the enlarged scale. Solid curves correspond to the best quality of fit to the data $\chi^2 = 2.4$.

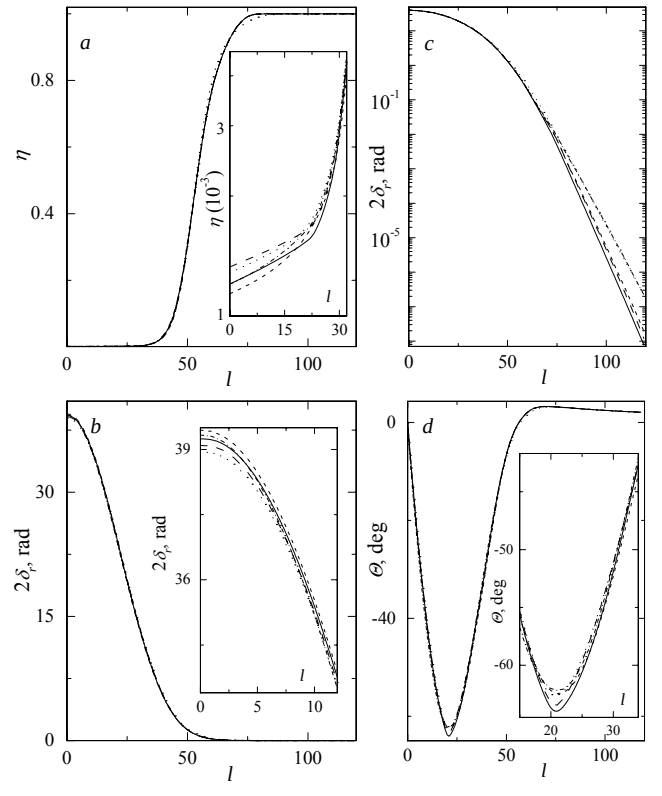

Fig. 2. The same as Fig. 1, but with primary model (5) for $S(l)$.

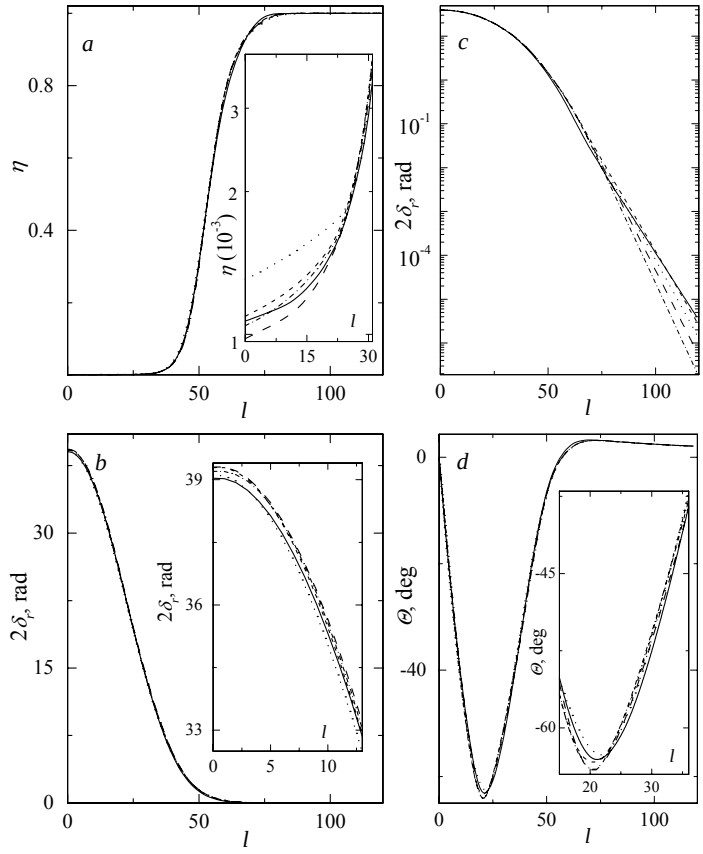

Fig. 3. The same as Fig. 1, but with primary model (6) for $S(l)$.

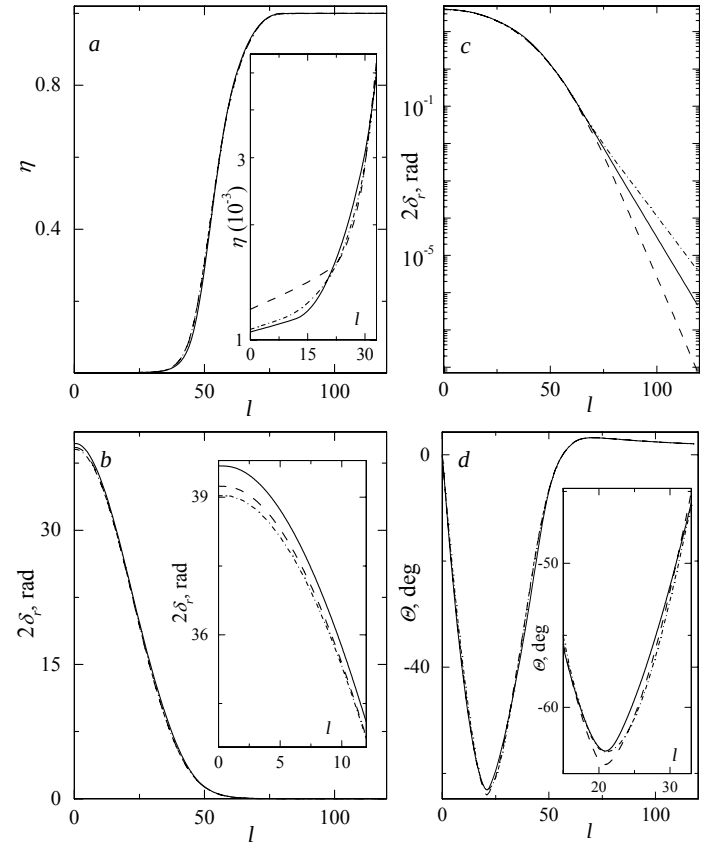

Fig. 4. Three best results from Figs. 1 - 3. Notation is the same as in Fig. 1.

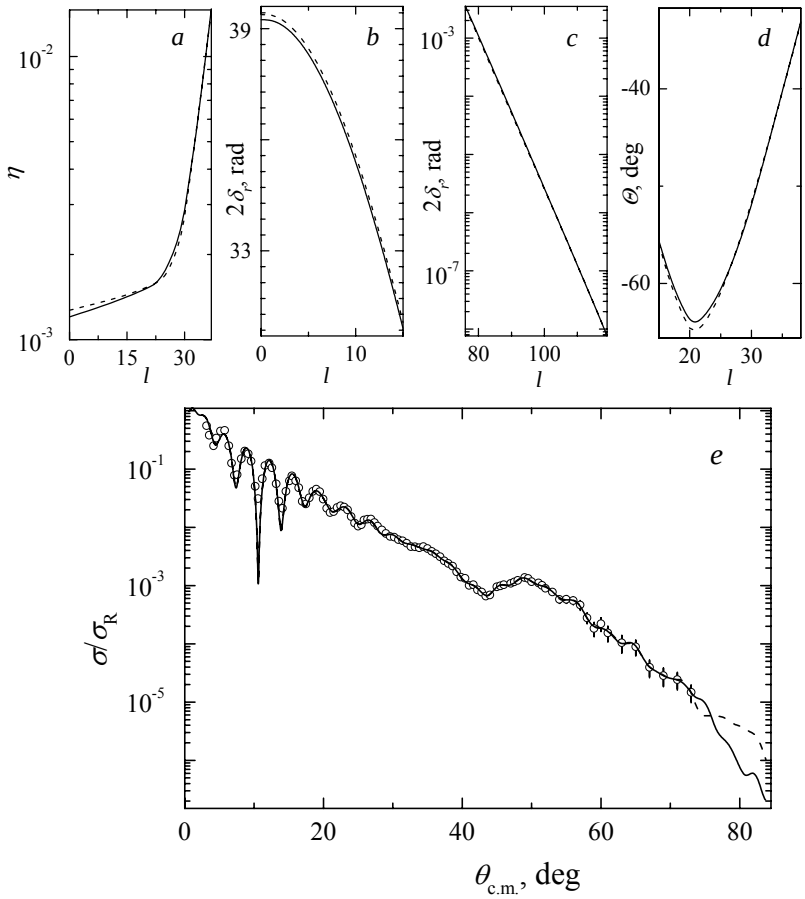

Fig. 5. Two scattering matrices and differential cross sections for the elastic ^{16}O - ^{16}O-scattering at 350 MeV, calculated by our procedure with primary model (5) for $S(l)$. Solid (dashed) curves are the results of calculations with the invented data points taken (not taken) into account in the region of large scattering angles. *a* and *b* – scattering matrix moduli $\eta(l)$ and nuclear phases $\delta_r(l)$ in the region of small momenta, respectively; *c* – the phases $\delta_r(l)$ in the region of large momenta; *d* – deflection functions $\Theta(l)$ in the vicinity of the minima; *e* – the differential cross sections (ratio to the Rutherford cross section). Experimental data are taken from [14, 15]. Solid curves presenting $S(l)$ correspond to the same ones shown in Fig. 2.

4. Discussion

The evolutionary procedure of determining the scattering matrix directly from the available experimental data on nucleus-nucleus elastic scattering cross sections at intermediate energies, presented in this article, is aimed at searching for the globally optimal solution. But, being aware of the complexity of the problem under study and the fact that the actual number of fitting parameters (twice the number of angular momenta, which is $l_{\max} = 120$ in our test case) is substantially greater than the actual number of data points (which is equal to 105 in our test case), we do not expect to achieve it. Therefore, we consider the obtained results (Figs. 1 - 5) as very promising.

First of all, we see that within every model representation used for the primary $S(l)$ dependence, regardless of the variety of their shapes, the moduli $\eta(l)$ and the nuclear refraction phases $\delta_r(l)$, as well as the total deflection functions $\Theta(l)$, obtained in different runs of the developed procedure, go close to each other (Figs. 1 - 3). The differences between them can sometimes be seen only in the enlarged or even logarithmic scale. The same observation can be made if one analyzes the compilation of the best results (Fig. 4), which points out their independence of the initial conditions.

At the same time, the nuclear phases $\delta_r(l)$ deviate from each other in the region of large angular momenta. There the scattering matrix module $\eta(l)$ are very close to unity, which makes the contributions of the partial waves with these values of l to the scattering amplitude vanishingly small. Nevertheless, we are able to conclude that,

under the requirements i) – v) imposed on the phases $\delta_{a,r}(l)$, we have managed to localize the region of the scattering matrix shapes that gives the lowest values to the χ^2 magnitude. It is somewhat surprising that the incorporation of the additional pseudo data points in the fitness function, which really forces the differential cross section to behave as desired, produces no noticeable corrections to the scattering matrix (Fig. 5) in the whole range of *l*. This is against the conventional way of thinking, but could be just a feature of that particular data set under study.

From the physics viewpoint, our results support the rainbow interpretation of the given data: the nuclear rainbow angle that corresponds to the minimum of the deflection function $\Theta(l)$ acquires the values θ_r = = 61 - 64°. If, from the very beginning, we abandon all requirements i) – v) imposed on the shapes of $\delta_{a,r}(l)$, then the procedure becomes able to find the results with χ^2 = 0.5 - 0.6. But the *S*-matrices for these cases are nonmonotonic and substantially different from run to run, belonging to different local optima.

5. Conclusion

The evolutionary procedure under description has been devised to determine the scattering matrix in the angular momentum representation. The similar approach can be used to develop the evolutionary procedure for the determination of radial dependence of a complex optical potential. With the help of this procedure, the optical potential can be extracted directly from the experimental data. Moreover, with the use of the similar procedure, the scattering matrix produced by the optical potential can be fitted to the scattering matrix extracted directly from the data. This means that the optical potential found in this way will correspond to the scattering matrix extracted immediately from the data. Having unified these three search procedures into one, we obtain a powerful tool for the deep theoretical investigation of heavy-ion collisions at intermediate energies.

REFERENCES

1. *McIntyre J.A., Wang K.H., Becker L.C.* Analysis of alpha-particle elastic scattering experiments // Phys. Rev. - 1960. - Vol. 117, No. 5. - P. 1337 - 1338.
2. *Berezhnoy Yu.A., Pilipenko V.V.* Analysis of refraction effects in nuclear scattering on the basis of the S-matrix approach // Mod. Phys. Lett. - 1995. - Vol. A10, No. 31. - P. 2305 - 2312.
3. *Berezhnoy Yu.A., Molev A.S.* Interference of diffractive, refractive and Coulomb effects in light nucleus-nucleus elastic scattering cross-sections at intermediate energies // Int. J. Mod. Phys. - 2003. - Vol. E12, No. 6. - P. 827 - 840.
4. *Kobos A.M., Brandan M.E., Satchler G.R.* Further optical model studies of ^{16}O scattering at *E/A* = 94 MeV // Nucl. Phys. - 1988. - Vol. A487, No. 3. - P. 457 - 476.
5. *Brandan M.E., McVoy K.W.* Rainbow-shift mechanism behind discrete optical-potential ambiguities // Phys. Rev. - 1991. - Vol. C43, No. 3. - P. 1140 - 1154.
6. *Allen L.J., Berge L., Steward C. et al.* An optical potential from inversion of the 350 MeV ^{16}O-^{16}O scattering data // Phys. Lett. - 1993. - Vol. B298, No. 1. - P. 36 - 40.
7. *Cooper S.G., McEwan M.A., Mackintosh R.S.* Elastic scattering phenomenology by inversion: ^{16}O on ^{12}C at 608 MeV // Phys. Rev. - 1992. - Vol. C45, No. 2. - P. 770 - 773.
8. *McEwan M.A., Cooper S.G., R.S. Mackintosh R.S.* Elastic-scattering phenomenology by inversion: (1). ^{12}C + ^{12}C from 140 to 2400 MeV // Nucl. Phys. - 1993. - Vol. A552, No. 2. - P. 401 - 436.
9. *Nicoli M.P., Haas F., Freeman R.M. et al.* Detailed study and mean field interpretation of ^{16}O + ^{12}C elastic scattering at seven medium energies // Phys. Rev. - 2000. - Vol. C61. - P. 034609.
10. *Ermer M., Clement H., Frank G. et al.* Model-unrestricted scattering potentials for light ions and their interpretation in the folding model // Phys. Lett. - 1989. - Vol. B224, No. 1, 2. - P. 40 - 44.
11. *Morris J.R., Deaven D.M., Ho K.M.* Genetic-algorithm energy minimization for point charges on a sphere // Phys. Rev. - 1996. - Vol. B53, No. 4. - P. R1740 - R1743.
12. *Winkler C., Hofmann H.M.* Determination of bound-state wave functions by a genetic algorithm // Phys. Rev. - 1997. - Vol. C55, No. 2. - P. 684 - 687.
13. *Brandan M.E., Satchler G.R.* Folding model analysis of ^{12,13}C + ^{12}C and ^{16}O + ^{12}C scattering at intermediate energies using a density-dependent interaction // Nucl. Phys. - 1988. - Vol. A487, No. 3 - P. 477 - 492.
14. *Stiliaris E., Bohlen H.G., Fröbrich P. et al.* Nuclear rainbow structures in the elastic scattering of ^{16}O on ^{16}O at E_L = = 350 MeV // Phys. Lett. - 1989. - Vol. B223, No. 3. - P. 291 - 295.
15. *Brandan M.E., Satchler G.R.* Optical potential ambiguities and ^{16}O + ^{16}O at 350 MeV // Phys. Lett. - 1991. - Vol. B256, No. 3, 4. - P. 311 - 315.

МОДЕЛЬНО-НЕЗАЛЕЖНИЙ ОПИС ПРУЖНОГО РОЗСІЯННЯ ЛЕГКИХ ЯДЕР ЯДРАМИ В ОБЛАСТІ ПРОМІЖНИХ ЕНЕРГІЙ

В. Ю. Корда, О. С. Молєв, Л. П. Корда

На основі еволюційного алгоритму розвинуто новий підхід, із застосуванням якого можна здобувати матрицю розсіяння $S(l)$ як комплексну функцію орбітального моменту l безпосередньо з експериментальних даних із пружного ядро-ядерного розсіяння при проміжних енергіях без залучення додаткових модельних припущень. Завдяки автоматичному контролю поведінки похідних $S(l)$ здобута матриця ^{16}O - ^{16}O-розсіяння при енергії 350 МеВ визначається модулем і ядерною фазою, які є плавними монотонними функціями орбітального моменту. Доведено, що кінцева форма $S(l)$ не залежить від початкових зображень матриці розсіяння, за які обиралися звичайно застосовувані феноменологічні моделі.

МОДЕЛЬНО-НЕЗАВИСИМОЕ ОПИСАНИЕ УПРУГОГО РАССЕЯНИЯ ЛЕГКИХ ЯДЕР ЯДРАМИ В ОБЛАСТИ ПРОМЕЖУТОЧНЫХ ЭНЕРГИЙ

В. Ю. Корда, А. С. Молев, Л. П. Корда

На основе эволюционного алгоритма развит новый подход, с использованием которого можно извлекать матрицу рассеяния $S(l)$ как комплексную функцию орбитального момента l непосредственно из экспериментальных данных по упругому ядро-ядерному рассеянию при промежуточных энергиях без привлечения дополнительных модельных предположений. Благодаря автоматическому контролю поведения производных $S(l)$ полученная матрица ^{16}O - ^{16}O-рассеяния при энергии 350 МэВ определяется модулем и ядерной фазой, являющимися плавными монотонными функциями орбитального момента. Показано, что конечная форма $S(l)$ не зависит от начальных представлений матрицы рассеяния, в качестве которых выбирались обычно используемые феноменологические модели.

Received 23.06.06,
revised - 18.06.07.